Extinction Limits of Nonadiabatic, Catalyst-Assisted Flames in Stagnation-Point Flow

Stephen B. Margolis and Timothy J. Gardner

Approved for public release; further dissemination unlimited.

Sandia National Laboratories

EXTINCTION LIMITS OF NONADIABATIC, CATALYST-ASSISTED FLAMES IN STAGNATION-POINT FLOW

Stephen B. Margolis[†] and Timothy J. Gardner[‡]

[†]Combustion Research Facility

Sandia National Laboratories

Livermore, California 94551-0969

[‡]Advanced Materials Laboratory

Sandia National Laboratories

Albuquerque, New Mexico 87185-1349

ABSTRACT

An idealized geometry corresponding to a premixed flame in stagnation-point flow is used to investigate the effects of catalysis on extending the extinction limits of nonadiabatic stretched flames. Specifically, a surface catalytic reaction is assumed to occur on the stagnation plane, thereby augmenting combustion in the bulk gas with an exothermic surface reaction characterized by a reduced activation energy. Assuming the activation energies remain large, an asymptotic analysis of the resulting flame structure yields a formula for the extinction limit as a function of various parameters. In particular, it is demonstrated that the presence of a surface catalyst can extend the burning regime, thus counterbalancing the effects of heat loss and flame stretch that tend to shrink it. The analysis is relevant to small-volume combustors, where the increased surface-to-volume ratio can lead to extinction of the nonadiabatic flame in the absence of a catalyst.

This page intentionally left blank

EXTINCTION LIMITS OF NONADIABATIC, CATALYST-ASSISTED FLAMES IN STAGNATION-POINT FLOW

1. Introduction

Because combustion is essentially an Arrhenius process, premixed flames generally can only exist within certain parameter ranges, or extinction limits, that correspond to a rate of heat production that is sufficient to sustain the reaction in a given flow geometry. Nonetheless, it is frequently desirable to extend these limits, often for the purpose of increasing fuel efficiency and/or reducing the rate of formation of pollutant species. Another emerging motivation is to allow combustion to be sustained in relatively small volumes, which are characterized by larger surface-to-volume ratios, that would otherwise lead to extinguishing levels of heat loss. Surface catalysts are widely used to achieve such enhancements with respect to efficiency and pollutant formation, and we wish to now consider the role catalysts might play with respect to nonadiabatic flames.

The model problem to be studied is illustrated in Figure 1, which depicts a nonadiabatic stretched flame in stagnation-point flow against a catalytic surface. This geometry is similar to that considered by others (*cf.* Law and Sivashinsky [1]; Giovangigli and Candel [2]; Warnatz *et al.* [3]), who have analyzed such a problem both analytically and numerically in the absence of heat losses. In addition to previous experimental investigations (*cf.* Law *et al.* [4]; Ikeda *et al.* [5]), this geometry is also suggested by more recent experiments (Gardner *et al.* [6]) on small-volume combustors. In the latter application, such a combustor (nominally $2500\mu \times 2500\mu \times 400\mu$) is fed by an inlet tube that blows against a catalytic surface (platinum mounted on a titanium/silicon wafer) and is vented by one or more outlet ports on either the opposite face (shortest dimension) or sides. In those experiments, it was demonstrated, following ignition by the heated catalytic surface, that a nearly flat flame could be sustained under the inlet port, close to the catalytic surface, without further heat addition. In the absence of the catalyst, the level of heat loss was apparently sufficient to extinguish the flame.

The purpose of the present work is to present an analysis of the model depicted in Figure 1 that takes into account the effects of nonadiabaticity. Specifically, solution-response curves, parameterized by a heat-loss coefficient and other parameters, are obtained that illustrate the extension of extinction limits arising from the additional catalytic surface reaction. The latter is assumed to proceed exothermically at reduced activation energy relative to the reaction in the bulk gas, and enables the flame to be sustained at higher rates of heat loss than would otherwise be the case.

2. Model Formulation

Referring to Figure 1, the stagnation-point flow is assumed to be cylindrically symmetric, occupying the domain $0 < \tilde{z} < \infty$, $0 < \tilde{r} < \infty$, where $\tilde{z}$ and $\tilde{r}$ are the axial and radial coordinates, respectively, and the tildes denote dimensional quantities. The catalytic surface, assumed adiabatic, thus corresponds to the plane $\tilde{z} = 0$, and the effects of heat loss arising from the remaining finite dimensions of an actual combustor are represented in a volumetric fashion. Although one may consider the portion of the flow field of interest to be governed by a boundary-layer formulation (*cf.* [1]), it turns out that qualitatively identical results are obtained (Section 4) if potential flow and weak thermal expansion are assumed. Accordingly, we make these assumptions for simplicity, resulting in the specified flow field $(\tilde{u}, \tilde{w}) = \tilde{\nabla}\tilde{\phi}$, where $\tilde{u}$ and $\tilde{w}$ are the radial and axial velocities, respectively, the velocity potential $\tilde{\phi} = -\tilde{a}(\tilde{z}^2 - \tilde{r}^2/2)$, and $\tilde{a}$ is the strain rate. Equivalently,

$$\tilde{u}(\tilde{r}, \tilde{z}) = -\frac{1}{\tilde{r}}\frac{\partial \tilde{\psi}}{\partial \tilde{z}} = \tilde{a}\tilde{r}\,, \quad \tilde{w}(\tilde{r}, \tilde{z}) = \frac{1}{\tilde{r}}\frac{\partial \tilde{\psi}}{\partial \tilde{r}} = -2\tilde{a}\tilde{z}\,, \quad \tilde{\psi} = -\tilde{a}\tilde{r}^2\tilde{z}\,, \tag{1}$$

where $\tilde{\psi}(\tilde{r}, \tilde{z})$ is the stream function.

Given this flow field, the conservation equations for the temperature $\tilde{T}$ and mass fraction Y of the deficient component of the mixture (*i.e.*, the mass fraction of fuel if the initial composition is lean, and the mass fraction of oxidizer if it is rich) are given in the region $0 < \tilde{z} < \infty$ by

$$\frac{\partial \tilde{T}}{\partial \tilde{t}} + \tilde{u}\frac{\partial \tilde{T}}{\partial \tilde{r}} + \tilde{w}\frac{\partial \tilde{T}}{\partial \tilde{z}} = \tilde{\lambda}\left[\frac{1}{\tilde{r}}\frac{\partial}{\partial \tilde{r}}\left(\tilde{r}\frac{\partial \tilde{T}}{\partial \tilde{r}}\right) + \frac{1}{r^2}\frac{\partial^2 \tilde{T}}{\partial \vartheta^2} + \frac{\partial^2 \tilde{T}}{\partial \tilde{z}^2}\right] + \tilde{Q}\tilde{A}_g Y^n e^{-\tilde{E}_g/\tilde{R}^\circ \tilde{T}} - \tilde{H}(\tilde{T} - \tilde{T}_u)\,, \tag{2}$$

$$\frac{\partial Y}{\partial \tilde{t}} + \tilde{u}\frac{\partial Y}{\partial \tilde{r}} + \tilde{w}\frac{\partial Y}{\partial \tilde{z}} = \tilde{\lambda}_m\left[\frac{1}{\tilde{r}}\frac{\partial}{\partial \tilde{r}}\left(\tilde{r}\frac{\partial Y}{\partial \tilde{r}}\right) + \frac{1}{r^2}\frac{\partial^2 Y}{\partial \vartheta^2} + \frac{\partial^2 Y}{\partial \tilde{z}^2}\right] - \tilde{A}_g Y^n e^{-\tilde{E}_g/\tilde{R}^\circ \tilde{T}}\,, \tag{3}$$

where ϑ is the angular coordinate, $\tilde{\lambda}$ and $\tilde{\lambda}_m$ are the thermal and mass diffusivities, respectively, $\tilde{Q}$ is the heat release (in units of temperature), $\tilde{A}_g$ and n are the rate coefficient and reaction order, $\tilde{E}_g$ is the activation energy of the gas-phase reaction, $\tilde{R}^\circ$ is the gas constant, and $\tilde{H}$ is the heat-loss rate coefficient. In writing the last term of Eq. (2), we have, for simplicity, represented heat losses in a standard volumetric/radiative fashion; an approximation for $\tilde{H}$ may be obtained from a knowledge of the corresponding surface heat-transfer coefficients and the surface-to-volume ratio of the combustor. The problem is closed by specifying the boundary conditions

$$\tilde{T} \to \tilde{T}_u\,, \quad Y \to Y_u \quad \text{as } z \to \infty\,, \tag{4}$$

$$\tilde{\lambda}\frac{\partial \tilde{T}}{\partial \tilde{z}}\bigg|_{z=0} = -\tilde{Q}\tilde{A}_s Y_s^n e^{-\tilde{E}_s/\tilde{R}^0 \tilde{T}_s}\,, \quad \tilde{\lambda}_m\frac{\partial Y}{\partial \tilde{z}}\bigg|_{z=0} = \tilde{A}_s Y_s^n e^{-\tilde{E}_s/\tilde{R}^0 \tilde{T}_s}\,, \tag{5}$$

where Y_s and $\tilde{T}_s$ represent values at $z = 0$ that are to be determined (it is assumed that the catalytic surface is highly conductive, so that T_s and Y_s are independent of r). The boundary conditions

6

(5) thus model the catalyst as an exothermic reaction at the surface $z = 0$, distinguished from the reaction rate in the bulk gas by a surface rate coefficient $\tilde{A}_s$ and a different activation energy $\tilde{E}_s$. It is assumed here that the catalytic surface is adiabatic, and thus all heat produced is conducted normal to the surface into the bulk gas (there is no convective contribution since $\tilde{w} = 0$ at the surface). The catalytic effect itself is modeled by assuming that $\tilde{E}_s < \tilde{E}_g$, thus allowing the surface reaction to take place at lower temperatures and consequently raising the temperature of the surrounding region such that the gas-phase reaction, if relatively weak in the absence of catalysis, is further encouraged.

As a basic solution of the problem just described, we seek steady, axisymmetric solutions that are functions of the axial coordinate z only, corresponding to the approximately planar flames that are typically observed in stagnation-point and counterflow configurations. We also introduce nondimensional quantities according to

$$z = \sqrt{\frac{\tilde{a}}{\tilde{\lambda}}}\, \tilde{z}, \quad y = \frac{Y}{Y_u}, \quad T = \frac{\tilde{T}}{\tilde{T}_u}, \quad Le = \frac{\tilde{\lambda}}{\tilde{\lambda}_m},$$

$$Q = \frac{\tilde{Q}}{\tilde{T}_u}, \quad H = \frac{\tilde{H}}{\tilde{a}}, \quad N_{g,s} = \frac{\tilde{E}_{g,s}}{\tilde{R}^\circ \tilde{T}_u}, \quad \nu = \frac{\tilde{E}_s}{\tilde{E}_g}. \tag{6}$$

In addition, we introduce the (unknown) characteristic flame temperature $\tilde{T}_f$ and the corresponding temperature "eigenvalue" Λ_s, where Λ_s, Λ_g and their ratio τ are defined as

$$\Lambda_s = \frac{\tilde{A}_s Y_u^n}{\sqrt{\tilde{a}\tilde{\lambda}}}\, e^{-\tilde{E}_s/\tilde{R}^\circ \tilde{T}_f}, \quad \Lambda_g = \frac{\tilde{A}_g Y_u^n}{\tilde{a}}\, e^{-\tilde{E}_g/\tilde{R}^\circ \tilde{T}_f}, \quad \tau = \frac{\Lambda_s}{\Lambda_g} = \sqrt{\frac{\tilde{a}}{\tilde{\lambda}}}\, \frac{\tilde{A}_s}{\tilde{A}_g}\, e^{(\tilde{E}_g - \tilde{E}_s)/\tilde{R}^\circ \tilde{T}_f}. \tag{7}$$

Thus, in terms of these nondimensional variables and parameters, steady, planar solutions of the problem are governed by

$$-2z\frac{dT}{dz} = \frac{d^2T}{dz^2} + Q\Lambda_g y^n\, e^{(N_g/T_f)(1 - T_f/T)} - H(T - 1), \quad 0 < z < \infty, \tag{8}$$

$$-2z\frac{dy}{dz} = Le^{-1}\frac{d^2y}{dz^2} - \Lambda_g y^n\, e^{(N_g/T_f)(1 - T_f/T)}, \quad 0 < z < \infty, \tag{9}$$

subject to

$$T \to 1, \quad Y \to 1 \quad \text{as } z \to \infty, \tag{10}$$

$$\left.\frac{dT}{dz}\right|_{z=0} = -Q\Lambda_s y_s^n\, e^{(N_s/T_f)(1 - T_f/T_s)}, \quad Le^{-1}\left.\frac{dy}{dz}\right|_{z=0} = \Lambda_s y_s^n\, e^{(N_s/T_f)(1 - T_f/T_s)}. \tag{11}$$

In what follows, we exploit the largeness of the activation-energy parameters N_g and N_s to obtain an asymptotic solution of Eqs. (8) – (11).

3. Asymptotic Analysis of the Model

Although we implicitly assume that $N_s < N_g$, which implies that the catalytic surface reaction can be sustained at lower temperatures than the distributed gas-phase reaction, it is reasonably assumed that both nondimensional activation energies are relatively large. Thus, their ratio ν, though less than unity, is still an O(1) quantity and, consequently, the bulk-gas and surface reactions will take place in close proximity to one another. In particular, since the catalytic surface is adiabatic and the surface reaction is exothermic, the peak temperature will be T_s and, at least near extinction, the thin distributed reaction zone will tend to lie adjacent to the catalytic surface.[1] In the outer region away from the surface, temperatures are sufficiently low that the reaction terms in Eqs. (8) and (9) become exponentially small.

In what follows, it will prove useful to introduce the large parameter β defined by

$$\beta = (N_g/T_f)(1 - 1/T_f),\tag{12}$$

which is proportional to the nondimensional activation energy. Based on previous asymptotic studies of nonadiabatic combustion problems (*cf.* Matkowsky and Olagunju [7]; Booty *et al.* [8]; Kaper *et al.* [9]; Margolis and Johnston [10]), it is clear that extinction then occurs for $O(\beta^{-1})$ values of the volumetric heat-loss coefficient H. Accordingly, we define the scaled parameter h, and, for further convenience, introduce a normalized temperature Θ and heat release q as

$$H = \beta^{-1}h,\quad \Theta = \frac{T-1}{T_f-1} = \frac{\tilde{T}-\tilde{T}_u}{\tilde{T}_f-\tilde{T}_u},\quad q = \frac{Q}{T_f-1} = \frac{\tilde{Q}}{\tilde{T}_f-\tilde{T}_u}\,.\tag{13}$$

In terms of these quantities, Eqs. (8) – (11) are expressed in a form suitable for asymptotic analysis as

$$-2z\frac{d\Theta}{dz} = \frac{d^2\Theta}{dz^2} + q\Lambda_g y^n\, e^{\beta(\Theta-1)/[T_f^{-1}+(1-T_f^{-1})\Theta]} - \beta^{-1}h\Theta,\quad 0 < z < \infty,\tag{14}$$

$$-2z\frac{dy}{dz} = Le^{-1}\frac{d^2y}{dz^2} - \Lambda_g y^n\, e^{\beta(\Theta-1)/[T_f^{-1}+(1-T_f^{-1})\Theta]},\quad 0 < z < \infty,\tag{15}$$

subject to

$$\Theta \to 0,\quad Y \to 1 \quad \text{as } z \to \infty,\tag{16}$$

$$
\begin{aligned}
\left.\frac{d\Theta}{dz}\right|_{z=0} &= -q\tau\Lambda_g y_s^n\, e^{\nu\beta(\Theta_s-1)/[T_f^{-1}+(1-T_f^{-1})\Theta_s]},\\
Le^{-1}\left.\frac{dy}{dz}\right|_{z=0} &= \tau\Lambda_g y_s^n\, e^{\nu\beta(\Theta_s-1)/[T_f^{-1}+(1-T_f^{-1})\Theta_s]}\,.
\end{aligned}\tag{17}
$$

---

[1]Based on the combined effects of the strained flow field and Lewis number on the leading-order flame temperature [see Eq. (31) below], it has been heuristically argued [1] that extinction will occur in this near-surface burning regime, rather than at O(1) flame-standoff distances, when $Le < 1$. However, the more complete analysis in [2] suggests more generally that the flame will lie adjacent to the stagnation surface prior to extinction either when the Lewis number is less than a critical value that is somewhat greater than unity, or when the activation-energy ratio $\nu < 1/2$, corresponding to a sufficiently low surface activation energy and hence a more active catalytic reaction.

Considering first the outer region, where z and $1 - \Theta$ are both O(1), we see that the reaction terms are exponentially negligible. The solution in this region, denoted by a superscript "(o)", is thus governed by the reactionless equations

$$-2z\frac{d\Theta^{(o)}}{dz} = \frac{d^2\Theta^{(o)}}{dz^2} - \beta^{-1}h\Theta^{(o)}\,, \quad -2z\frac{dy^{(o)}}{dz} = Le^{-1}\frac{d^2y^{(o)}}{dz^2}\,, \tag{18}$$

subject to the outer boundary conditions (16) and appropriate matching conditions with the inner solution considered below. The appearance of the small parameter β^{-1} in the first of Eqs. (18) then suggests that the outer solutions be sought sought in the expanded form

$$\Theta^{(o)} \sim \Theta_0(z) + \beta^{-1}\Theta_1(z) + \cdots\,, \quad y^{(o)} \sim y_0(z) + \beta^{-1}y_1(z) + \cdots\,. \tag{19}$$

The leading-order solutions for Θ_0 and y_0 are then determined by the homogeneous version of Eqs. (18) and the boundary conditions (16) as

$$\Theta_0(z) = A_0 \operatorname{erfc}(z)\,, \quad y_0(z) = 1 + B_0 \operatorname{erfc}\left(\sqrt{Le}\,z\right)\,, \tag{20}$$

where the constants of integration A_0 and B_0 are to be determined from the matching conditions. At higher orders, the equations for y_i, $i \geq 1$, remain homogeneous, and the solutions, subject to $y_i = 0$ at $z = \infty$, are thus given by

$$y_i(z) = B_i \operatorname{erfc}\left(\sqrt{Le}\,z\right)\,, \quad i \geq 1\,. \tag{21}$$

However, because $y_0(z)$ is an exact solution of the second of Eqs. (20), we may, without loss of generality, set B_i, and hence y_i, to zero for $i \geq 1$. On the other hand, the inhomogeneous equation determining the next-order solution Θ_1 is given by

$$-2z\frac{d\Theta_1}{dz} = \frac{d^2\Theta_1}{dz^2} - h\Theta_0\,, \tag{22}$$

subject to $\Theta_1 = 0$ at $z = \infty$. Substituting the expression in Eq. (20) for Θ_0, the solution for Θ_1 can be obtained directly through successive integrations as

$$\Theta_1 = A_1 \operatorname{erfc}(z) - hA_0 \int_z^\infty e^{-\hat{z}^2}d\hat{z} \int_0^{\hat{z}} e^{\bar{z}^2}\operatorname{erfc}(\bar{z})\,d\bar{z}\,, \tag{23}$$

where A_1 is another as-yet-undetermined constant of integration. Reversing the order of integration in the double integral of Eq. (23) and dividing the integration domain into two parts, this result can be rewritten as

$$\begin{aligned}
\Theta_1(z) &= A_1 \operatorname{erfc}(z) - hA_0 \left[\int_z^\infty e^{\bar{z}^2}\operatorname{erfc}(\bar{z})\,d\bar{z} \int_{\bar{z}}^\infty e^{-\hat{z}^2}d\hat{z} + \int_0^z e^{\bar{z}^2}\operatorname{erfc}(\bar{z})\,d\bar{z} \int_z^\infty e^{-\hat{z}^2}d\hat{z} \right] \\
&= A_1 \operatorname{erfc}(z) - hA_0\frac{\sqrt{\pi}}{2} \left[\int_z^\infty e^{\bar{z}^2}\operatorname{erfc}^2(\bar{z})\,d\bar{z} + \operatorname{erfc}(z) \int_0^z e^{\bar{z}^2}\operatorname{erfc}(\bar{z})\,d\bar{z} \right]\,,
\end{aligned} \tag{24}$$

9

which consists of only single integrals. The final result (24) is recognized as the variation-of-parameters form of the solution.

The outer solutions $y^{(o)}(z; Le) = y_0(z)$ and $\Theta^{(o)}(z, H) \approx \Theta_0(z) + \beta^{-1}\Theta_1(z)$, along with the leading- and first-order temperature profiles $\Theta_0(z)$ and $\Theta_1(z)$, are exhibited in Figure 2. In plotting these solutions, we have used the fact that $\beta^{-1}h = H$ and the results, obtained from the analysis of the inner problem given below, that $A_0 = -B_0 = 1$ and $A_1 = 0$.

Having thus constructed two terms of the outer solution, we now consider the inner problem by introducing the stretched coordinate $\eta = \beta z$. In this thin region, which lies adjacent to the catalytic surface and in which chemical reaction becomes appreciable, Θ is within $O(\beta^{-1})$ of unity, as is Θ_s. We thus seek inner solutions, denoted by a superscript "(i)", in the expanded form

$$\Theta^{(i)} \sim 1 + \beta^{-1}\theta_1 + \epsilon^2\theta_2 + \cdots , \quad y^{(i)} \sim \beta^{-1}\zeta_1 + \beta^{-2}\zeta_2 + \cdots , \tag{25}$$

which implies $\Theta_s \sim 1 + \beta^{-1}\theta_s + \cdots$, with the surface-temperature coefficient θ_s to be determined. A leading-order balance of reactive and diffusive terms then implies the additional scalings

$$\Lambda_g = \beta^{(n+1)}\hat{\lambda}, \quad \tau = \beta^{-1}\hat{\tau}. \tag{26}$$

Substituting the inner expansions/scalings (25) and (26) into Eqs. (14), (15) and (17), the leading-order problem in the region $\eta > 0$ is determined as

$$0 = \frac{d^2\theta_1}{d\eta^2} + q\hat{\lambda}\zeta_1^n e^{\theta_1}, \quad 0 = Le^{-1}\frac{d^2\zeta_1}{d\eta^2} - \hat{\lambda}\zeta_1^n e^{\theta_1}, \tag{27}$$

subject to the boundary and matching conditions

$$\left.\frac{d\theta_1}{d\eta}\right|_{\eta=0} = -q\hat{\tau}\hat{\lambda}\zeta_s^n e^{\nu\theta_s}, \quad Le^{-1}\left.\frac{d\zeta_1}{d\eta}\right|_{\eta=0} = \hat{\tau}\hat{\lambda}\zeta_s^n e^{\nu\theta_s}, \tag{28}$$

$$0 = y_0\big|_{z=0}, \quad 1 = \Theta_0\big|_{z=0}, \quad \theta_1 \sim \Theta_1\big|_{z=0} + \eta\left.\frac{d\Theta_0}{dz}\right|_{z=0}, \quad \zeta_1 \sim \eta\left.\frac{dy_0}{dz}\right|_{z=0} \quad \text{as } \eta \to \infty. \tag{29}$$

We note that the first two of Eqs. (29) are actually the zeroth order matching conditions which determine the constants A_0 and B_0 in Eqs. (20) as $A_0 = 1$, $B_0 = -1$.

The solution of Eqs. (27) – (29) proceeds as follows. Adding the first and q times the second of Eqs. (27) gives, after integrating once and evaluating the constant of integration at $\eta = 0$ according to Eqs. (28), the result

$$\frac{d\theta_1}{d\eta} + Le^{-1}q\frac{d\zeta_1}{d\eta} = 0. \tag{30}$$

Substituting the matching conditions (29) into this result thus requires, according to Eq. (20) with the above values of A_0 and B_0, that $q/\sqrt{Le} = 1$. Thus, from the definition of q in Eq. (13),

$$T_f = 1 + Q/\sqrt{Le}, \tag{31}$$

10

which determines the reference flame temperature T_f, and hence Λ_s and Λ_g. We observe that unlike freely-propagating flames, the flame temperature of the stagnation-point flame depends on Lewis number, and is equal to the classical adiabatic flame temperature $T_f = 1 + Q$ only for $Le = 1$. The fact that T_f varies with Lewis number stems from the fact that the flame is stretched; i.e., the streamlines are divergent with respect to the flame normal. In particular, thermal and mass diffusion occur in the normal direction with respect to the flame, where thermal diffusion conducts heat away from the reaction zone into the preheat region and mass diffusion supplies chemical energy to the reaction zone from this region. Consequently, an increase (decrease) in Lewis number results in a net enthalpy loss (gain) to the flame with respect to the diverging flow, and hence a decrease (increase) in the flame temperature. However, it turns out that a lower leading-order flame temperature results in a greater sensitivity to surface catalysis since there is less conversion of the reactants in the bulk gas. Indeed, as indicated by Eq. (33) below, a larger Lewis number results in a greater reactant concentration at the catalytic surface, and hence the existence of a catalytic surface reaction will have a greater influence on the solution response in that case.

A second integration of Eq. (30) gives, again using the matching conditions (29), the relation

$$\theta_1 + Le^{-1}q\zeta_1 = A_1 - h\gamma\sqrt{\pi}/2\,, \quad \gamma = \int_0^\infty e^{\bar{z}^2}\mathrm{erfc}^2(\bar{z})\,d\bar{z} \doteq 0.391066\,, \tag{32}$$

where we have used the fact that $A_0 = 1$. Application of the matching conditions at the next order in the inner analysis, described in the Appendix, then determines that $A_1 = 0$, thus giving a determinate relationship between θ_1 and ζ_1. Consequently, from the result above Eq. (31),

$$\zeta_1 = \sqrt{Le}\big(-h\gamma\sqrt{\pi}/2 - \theta\big)\,, \tag{33}$$

and substituting this expression for ζ_1 into the first of Eqs. (27), an equation for θ_1 alone is obtained as

$$0 = \frac{d^2\theta_1}{d\eta^2} + \hat{\lambda}Le^{(n+1)/2}(-\theta_1 - c)^n e^{\theta_1}\,, \quad c = h\gamma\sqrt{\pi}/2\,. \tag{34}$$

This in turn may be integrated once to give

$$\frac{1}{2}\left(\frac{d\theta_1}{d\eta}\right)^2 + \hat{\lambda}Le^{(n+1)/2}\int_{-\infty}^{\theta_1}(-\bar{\theta}_1 - c)^n e^{\bar{\theta}_1}\,d\bar{\theta}_1 = \frac{2}{\pi}\,, \tag{35}$$

where the constant of integration was obtained from the matching condition (29) for θ_1. At this point, evaluation Eq. (34) at $\eta = 0$ according to the first of Eqs. (28) gives the condition

$$\frac{2}{\pi\hat{\lambda}} = Le^{(n+1)/2}\left[G_n(\theta_s; h) + \frac{1}{2}Le^{(n+1)/2}\hat{\tau}^2\hat{\lambda}\big(-\theta_s - \gamma h\sqrt{\pi}/2\big)^{2n}e^{2\nu\theta_s}\right]\,, \tag{36}$$

where $G_n(\theta_s; h)$ is defined as

$$G_n(\theta_s; h) = \int_{-\infty}^{\theta_s}\big(-\bar{\theta}_1 - \gamma h\sqrt{\pi}/2\big)^n e^{\bar{\theta}_1}\,d\bar{\theta}_1 = \int_{-\theta_s}^\infty\big(u - \gamma h\sqrt{\pi}/2\big)^n e^{-u}\,du\,. \tag{37}$$

11

Equation (36) thus determines the surface-temperature coefficient θ_s, which, through the definition of the temperature variable Θ in Eq. (13), determines the leading-order perturbation in the normalized surface temperature T_s relative to the characteristic, or zeroth order, flame temperature T_f given by Eq. (31). As discussed in detail in the following section, Equation (36) also admits a physical solution for θ_s only for parameter values that do not exceed a critical condition, and thus Eq. (36) defines an extinction criterion beyond which the present solution does not exist.

4. Extinction Limits

The integral represented by $G_n(\theta_s; h)$ can be evaluated explicitly for integer values of the reaction order n. Thus, for the first several integer values of n, we obtain

$$
\begin{aligned}
n = 0: \quad & G_0(\theta_s; h) = e^{\theta_s}, \\
n = 1: \quad & G_1(\theta_s; h) = \left(1 - \theta_s - \gamma h \sqrt{\pi}/2\right)e^{\theta_s}, \\
n = 2: \quad & G_2(\theta_s; h) = \left[1 + \left(1 - \theta_s - \gamma h \sqrt{\pi}/2\right)^2\right]e^{\theta_s}, \\
n = 3: \quad & G_3(\theta_s; h) = \left[2 + 3\left(1 - \theta_s - \gamma h \sqrt{\pi}/2\right) + \left(1 - \theta_s - \gamma h \sqrt{\pi}/2\right)^3\right]e^{\theta_s}.
\end{aligned}
\tag{38}
$$

We note that the result (35), in the absence of heat loss ($h = 0$) and with $n = 1$, essentially recovers that given in [1]. The only difference is that the left-hand side of Eq. (36), which results from the matching of $d\theta_1/d\eta$ in the limit $\eta \to \infty$ with the potential stagnation-point flow assumed here, is replaced with a different constant, expressed as an integral, that arises from the boundary-layer nature of the outer flow that was considered in that study. Thus, the solution-response curves obtained here, in the limit $h = 0$ and $n = 1$, are identical in form to those previous results.

Although physically we regard Equation (36) as an implicit equation for θ_s, it is computationally more convenient to define the two parameters α_1 and α_2 according to

$$
\alpha_1 = \frac{2}{\pi \hat{\lambda}}, \quad \alpha_2 = \frac{1}{2}\hat{\tau}^2 \hat{\lambda},
\tag{39}
$$

and to calculate α_1 as an explicit function of θ_s for various values of α_2 and the remaining parameters. Here, α_1, being inversely proportional to $\hat{\lambda}$ and hence Λ_g, may be regarded, according to the definition (7) of Λ_g, as a measure of either the strain rate $\tilde{a}$ or the reciprocal of the gas-phase reaction rate. Similarly, α_2, which is proportional to $\hat{\tau}^2\hat{\lambda}$, or to $(\Lambda_s/\Lambda_g)^2\Lambda_g$, is independent of $\tilde{a}$, but does represent a relative measure of the surface reaction rate with respect to that of the bulk gas (in units of the gas-phase rate). The remaining parameters of interest, h, ν, n and Le, are proportional to the rate of volumetric heat loss, the ratio of the surface activation energy to that of the gas-phase reaction, the reaction order and the ratio of the thermal to mass diffusivities, respectively.

We first analyze the results for the non-catalytic problem ($\alpha_2 = 0$). For $n = 1$, Eq. (36) thus becomes

$$
\frac{\alpha_1}{Le} = \left(1 - \theta_s - \gamma h \sqrt{\pi}/2\right)e^{\theta_s}, \quad n = 1,
\tag{40}
$$

where, from Eq. (33) and the fact that the inner mass-fraction variable ζ_1 is nonnegative, physical solutions are always restricted to $-\theta_s \geq h\gamma\sqrt{\pi}/2$, the lower limit corresponding to complete consumption of reactants by the gas-phase reaction (in which case $\zeta_s = 0$). The solution curve $\alpha_1(-\theta_s)$ is shown in Figure 3a, where we observe that no steady, planar solution exists for $\alpha_1/Le > e^{-\gamma h\sqrt{\pi}/2}$. Thus, we interpret this critical value of the strain-rate parameter α_1 as an extinction limit, a limit that is proportional to the Lewis number Le and which decreases exponentially with increasing values of the heat-loss parameter h. With respect to h, the critical condition for extinction is thus $\gamma h > (2/\sqrt{\pi})\ln(Le/\alpha_1)$, so that smaller values of the strain rate allow the flame to tolerate larger heat losses. We note that with respect to the parameter α_1, the flame is either more or less resistant to extinction, depending respectively on whether $Le > 1$ or $Le < 1$. The corresponding results for $n = 2$, which are obtained from

$$\frac{\alpha_1}{Le^{3/2}} = \left[1 + \left(1 - \theta_s - \gamma h\sqrt{\pi}/2\right)^2\right]e^{\theta_s}, \quad n = 2, \tag{41}$$

are exhibited in Figure 3b. We observe that the criterion for extinction in this case is $\alpha_1/Le^{3/2} > 2\,e^{-\gamma h\sqrt{\pi}/2}$ or, in terms of h, $\gamma h > (2/\sqrt{\pi})\ln(2\,Le^{3/2}/\alpha_1)$. Thus, relative to the $n = 1$ case, the flame is more resistant to the extinguishing effects of strain and heat loss for $2\,Le^{1/2} > 1$ (i.e., $Le > \sqrt{2}/2$), but is more prone to extinction for Lewis numbers smaller than this value.

Turning attention to the catalytic problem ($\alpha_2 > 0$), we consider in detail the case in which the overall reaction order n is unity. Thus, for $n = 1$, Eq. (36) determines the solution response according to

$$\frac{\alpha_1}{Le} = \left(1 - \theta_s - \gamma h\sqrt{\pi}/2\right)e^{\theta_s} + \alpha_2 Le(-\theta_s - \gamma h\sqrt{\pi}/2)^2 e^{2\nu\theta_s}, \quad n = 1, \tag{42}$$

where, as always, physical solutions are restricted to $-\theta_s \geq h\gamma\sqrt{\pi}/2$. In order to analyze the solution response, it is useful to first calculate $d\alpha_1/d(-\theta_s)$, which is given by

$$\frac{d\alpha_1}{d(-\theta_s)} = Le\left[(-\theta_s) - \gamma h\sqrt{\pi}/2\right]e^{-(-\theta_s)}\left[-1 + 2\alpha_2 Le\left\{1 - \nu\left[(-\theta_s) - \gamma h\sqrt{\pi}/2\right]\right\}e^{(1-2\nu)(-\theta_s)}\right]. \tag{43}$$

Thus, the equation $d\alpha_1/d(-\theta_s) = 0$ always has a root at $-\theta_s = \gamma h\sqrt{\pi}/2$, corresponding to $\alpha_1/Le = e^{-\gamma h\sqrt{\pi}/2}$, and may have additional physical roots(s) at value(s) of $-\theta_s$ that satisfy the condition

$$2\alpha_2 Le\left\{1 - \nu\left[(-\theta_s) - \gamma h\sqrt{\pi}/2\right]\right\} = e^{(2\nu-1)(-\theta_s)}. \tag{44}$$

For example, if $\nu = 1/2$, corresponding to the case in which the activation energy of the catalytic surface reaction is half that of the distributed reaction in the bulk gas, Eq. (44) is satisfied when $-\theta_s = \gamma h\sqrt{\pi}/2 + \delta$, where $\delta = (2\alpha_2 Le - 1)/(\alpha_2 Le)$. Thus, for $\alpha_2 Le > 1/2$ (i.e., for $\delta > 0$), there exists a physical root of Eq. (44) corresponding to $\alpha_1 = \alpha_1^e = Le(1 + \delta + \alpha_2 Le\delta^2)e^{-\gamma h\sqrt{\pi}/2-\delta}$. On

the other hand, for $\alpha_2 Le < 1/2$ (*i.e.*, for $\delta < 0$), this additional root is unphysical since it occurs for $-\theta_s < \gamma h \sqrt{\pi}/2$.

The consequences of a physical root of Eq. (44) are clear from Figures 4a and 4b, which are drawn for the case $\nu = 1/2$ just described. For $\alpha_2 Le > 1/2$, corresponding to a sufficiently vigorous surface reaction, the extinction limit is increased (since $d^2\alpha_1/d(-\theta_s)^2\big|_{-\theta_s=\gamma h\sqrt{\pi}/2} > 0$) to the value $\alpha_1 = \alpha_1^e$ given above (Figure 4a). In addition, the solution becomes multi-valued for $Le \cdot e^{-\gamma h\sqrt{\pi}/2} < \alpha_1 < \alpha_1^e$, implying both a high- and low-temperature solution (corresponding to a small and large value of $-\theta_s$, respectively) for α_1 within this range. On the other hand, for $\alpha_2 Le < 1/2$ (Figure 4b), which corresponds to a relatively weak surface reaction, the extinction limit $\alpha_1 = Le \cdot e^{-\gamma h\sqrt{\pi}/2}$ remains the same as that in the absence of a catalytic reaction altogether. That is, even though a weak catalytic reaction does modify the solution response relative to the noncatalytic case, the maximum possible value of α_1 is unchanged. This can be seen from a comparison of Figures 3a and 4b, which were drawn for the same value of h and $Le = 1$. In physical terms, the effects of a sufficiently active surface reaction at a reduced activation energy allows for a lower peak flame temperature (*i.e.*, a larger value of $-\theta_s$, which, according to Eq. (33), is required to accommodate a larger value of ζ_s), thereby extending the extinction limit. This corresponds to the fact that reactants which leak through the gas-phase reaction region are still able to undergo conversion at the catalytic surface. If the catalytic reaction is weak or absent altogether, this additional opportunity for reaction is reduced or eliminated, and consequently, the gas flame cannot sustain itself at higher values of the strain-rate parameter α_1 than can be tolerated in the noncatalytic case. In terms of the heat-loss parameter h, the critical value corresponding to extinction is raised to $\gamma h = \gamma h^e = (2/\sqrt{\pi})\big[\ln(Le/\alpha_1) + \ln(1 + \delta + \alpha_2 Le\delta^2) - \delta\big]$. As $\delta \downarrow 0$ (*i.e.*, as $\alpha_2 Le \downarrow 1/2$), the maximum rate of heat loss that can be tolerated for a given value of α_1 is reduced to the previous limit given above for the noncatalytic problem.

Extending these results beyond the special case $\nu = 1/2$, we observe from differentiating Eq. (43) that

$$\frac{d^2\alpha_1}{d(-\theta_s)^2}\bigg|_{-\theta_s=\gamma h\sqrt{\pi}/2} = Le \cdot e^{-\gamma h\sqrt{\pi}/2}\left[2\alpha_2 Le \cdot e^{(1-2\nu)\gamma h\sqrt{\pi}/2} - 1\right]. \qquad (45)$$

Thus, at the smallest physical value for $-\theta_s$, namely $-\theta_s = -\theta_s^0 = \gamma h\sqrt{\pi}/2$, $d^2\alpha_1/d(-\theta_s)^2$ is either positive or negative depending on whether $2\alpha_2 Le$ is greater or less than $e^{(2\nu-1)h\gamma\sqrt{\pi}/2}$. In the first case, since $d\alpha_1/d(-\theta_s)$ is zero at $-\theta_s^0$, α_1 will increase with increasing $-\theta_s$ until it reaches a maximum at the value of $-\theta_s$ given by the single root of Eq. (44). This argument holds for all values of ν since, at $-\theta_s = -\theta_s^0$, the left-hand side of Eq. (44) exceeds the value of the righthand side, leading to a single intersection when the linear left-hand and exponential right-hand sides of Eq. (44) are plotted against $-\theta_s$. Consequently, for $2\alpha_2 Le > e^{(2\nu-1)h\gamma\sqrt{\pi}/2}$, the qualitative behavior will be identical to Figure 4a, indicating an extension of the extinction limit as described above.

14

On the other hand, for the case $2\alpha_2 Le < e^{(2\nu-1)h\gamma\sqrt{\pi}/2}$, corresponding to a negative value of $d^2\alpha_1/d(-\theta_s)^2$ at $-\theta_1 = -\theta_s^0$ and hence a decrease in α_1 as $-\theta_s$ increases from that value, the qualitative nature of the solution response depends on whether ν is greater or less than $1/2$. If $\nu \geq 1/2$, the right-hand side of Eq. (44) is either exponentially increasing or constant, whereas the left-hand side is a linearly decreasing function of $-\theta_s$. In this case, since the left-hand side of Eq. (44) is less than the value of the righthand side at $-\theta_s = -\theta_s^0$, there are no physical roots of Eq. (44), the solution response is qualitatively similar to Figure 4b, and there is no catalytic extension of the extinction limit. This situation persists as ν decreases below the value $1/2$ (in which case the right-hand side of Eq. (44) becomes a decaying exponential) until at some point the linearly decreasing left-hand side of Eq. (44) intersects the exponentially-decaying right-hand side tangentially in at first one, and then two places. The first of these roots, if it occurs for $-\theta_s > -\theta_s^0$, then corresponds to a relative minimum in the $\alpha_1(-\theta_s)$ response, while the second corresponds to a relative maximum and hence an extension of the extinction limit due to surface catalysis (provided this root occurs in the physical range $-\theta_s > -\theta_s^0$ and the relative maximum value of α_1 exceeds the value at $-\theta_s^0$). We observe that in the two-root case just described, the solution response is triple-valued for a range of α_1 values, corresponding to low-, intermediate- and high-temperature solution branches.

The various scenarios just described for $\nu < 1/2$, which illustrate how different effects can counterbalance one another, are illustrated in Figures 5a–e. In particular, the $h = 0$ curve in Figure 5a demonstrates both the aforementioned relative minimum and maximum for $2\alpha_2 Le < e^{(2\nu-1)h\gamma\sqrt{\pi}/2}$, while the other two curves for $h > 0$ exhibit only the relative maximum in the physical range $-\theta_s > -\theta^0$ as the decrease in h eventually leads to the parameter regime $2\alpha_2 Le > e^{(2\nu-1)h\gamma\sqrt{\pi}/2}$. In Figure 5b, which is qualitatitively similar to Figure 5a, the surface activation-energy parameter ν has been decreased further with respect to its previous value, leading to a greater catalytic effect and a consequently greater extension of the extinction limit. This same effect is achieved by increasing the surface reaction-rate parameter α_2 to the value used in Figure 5c, where there is now no relative minimum in any of the solution responses since the value of $\alpha_2 Le$ is now sufficiently large that $2\alpha_2 Le > e^{(2\nu-1)h\gamma\sqrt{\pi}/2}$ for all $h \geq 0$. Hence, decreasing ν and increasing α_2 have the same qualitative effect on the extension of the extinction limit. Finally, the effects of Lewis number on the solution response in the present case is shown in Figures 5d and 5e, corresponding to Lewis numbers less than and greater than unity, respectively. Figures 5d and 5e are qualitatively similar to Figure 5a, which depicts the unity Lewis-number case for the same values of the remaining parameters. Comparison of these three figures shows that smaller Lewis numbers, which correspond to an increase in the leading-order flame temperature and a reduced catalytic influence arising from a lower surface reactant concentration, as described below Eq. (31), result in less of an extension of the extinction limit. Larger Lewis numbers, on the

other hand, correspond to a decrease in T_f, a larger surface reactant concentration, and thus an enhanced catalytic effect that leads to a greater extension of the extinction limit. Consequently, relative to the noncatalytic problem, the positive effects of catalysis in extending the extinction limit are enhanced for larger Lewis-number flames.

5. Conclusion

The present analysis has shown that in a fundamental strained-flame geometry, the presence of a catalytic surface has the potential to significantly extend the extinction limits arising from the effects of flame stretch and heat loss. In particular, reactants that leak through the distributed portion of the gas flame due to either larger strain rates and/or larger rates of heat loss that lower the reaction rate, have an additional opportunity to react under the influence of a catalyst at the surface. Such an influence is particularly desirable from the standpoint of building small combustors with dimensions on the order of a millimeter or less. Such combustors have correspondingly larger surface-to-volume ratios, and the present work has therefore focused on extending earlier studies to the nonadiabatic regime. Recent experiments suggest that combustors with dimensions under a millimeter can support a self-sustaining flame when one of the walls acts as a catalytic surface.

The solution response of the model problem has been displayed as a plot of a surface-temperature perturbation versus a rate-of-strain parameter, for various values of a volumetric heat-loss coefficient and other parameters of interest. The results clearly demonstrate how, in certain parameter regimes associated with a strongly catalytic effect, the solution response is modified from the noncatalytic case to allow for a larger value of the strain rate and/or rate of heat loss than would be the case in the absence of catalysis. In addition, it was shown that although larger Lewis numbers, corresponding to less mobile (heavier) reactants that have reduced ability to diffuse across the streamlines of the divergent flow, lead to a lowering of the flame temperature in the absence of catalysis, the effect of a catalyst becomes more significant for such Lewis numbers once reactants are convectively transported to the vicinity of the catalytic surface. In such cases, the solution response exhibits an extinction limit at a value of the strain rate (or heat-loss coefficient) that is larger than the corresponding value in the absence of catalysis, resulting in a catalytic extension of the extinction limit.

Appendix

The determination that $A_1 = 0$ in Eq. (32) follows from a consideration of the next-order inner problem for θ_2 and ζ_2 in the expansions (25). That problem, obtained from Eqs. (14), (15) and (17), is given by

$$0 = \frac{d^2\theta_2}{d\eta^2} + q\hat{\lambda} f(\zeta_1, \zeta_2, \theta_1, \theta_2; n) e^{\theta_1}, \quad 0 = Le^{-1}\frac{d^2\zeta_2}{d\eta^2} - \hat{\lambda} f(\zeta_1, \zeta_2, \theta_1, \theta_2; n) e^{\theta_1}, \qquad (A.1)$$

subject to the matching conditions

$$\theta_2 \sim \Theta_2\big|_{z=0} + \eta\frac{d\Theta_1}{dz}\bigg|_{z=0} + \frac{1}{2}\eta^2\frac{d^2\Theta_0}{dz^2}\bigg|_{z=0}, \quad \zeta_2 \sim \frac{1}{2}\eta^2\frac{d^2y_0}{dz^2}\bigg|_{z=0} \quad \text{as } \eta \to \infty. \tag{A.2}$$

and the boundary conditions

$$\frac{d\theta_2}{d\eta}\bigg|_{\eta=0} = -q\hat{\tau}\hat{\lambda}_0 f(\zeta_s, \hat{\zeta}_s, \theta_s, \hat{\theta}_s; n)\, e^{\nu\theta_s}, \quad Le^{-1}\frac{d\zeta_2}{d\hat{\eta}}\bigg|_{\eta=0} = \hat{\tau}\hat{\lambda}f(\zeta_s, \hat{\zeta}_s, \theta_s, \hat{\theta}_s; n)\, e^{\nu\theta_s}, \tag{A.3}$$

where $\hat{\zeta}_s = \zeta_2\big|_{\eta=0}$, $\hat{\theta}_s = \theta_2\big|_{\eta=0}$, and $f(\zeta_1, \zeta_2, \theta_1, \theta_2; n) = \zeta_2^n + \zeta_1^{n-1}\big[\theta_2 - (1-\sigma)\theta_1^2\big]$.

Adding the first and q times the second of Eqs. (A.1), integrating once, and using Eqs. (A.3) to evaluate the constant of integration, we obtain

$$\frac{d\theta_2}{d\eta} + Le^{-1}q\frac{d\zeta_2}{d\eta} = 0. \tag{A.4}$$

The left-hand side of Eq. (A.4) may now be evaluated for large η according to the matching conditions (A.2). From the outer solution given by Eqs. (20) and (24), we calculate $d\Theta_1/dz\big|_{z=0} = -2A_1/\sqrt{\pi}$ and $d^2\Theta_0/dz^2\big|_{z=0} = d^2y_0/dz^2\big|_{z=0} = 0$. Consequently, we obtain from Eq. (A.4) evaluated at $\eta = \infty$ the result $A_1 = 0$.

Acknowledgment

References

[1] Law, C. K., and Sivashinsky, G. I., "Catalytic Extension of Extinction Limits of Stretched Premixed Flames," *Combustion Science and Technology*, Vol. 29, 1982, pp. 277–286.

[2] Giovangigli, V., and Candel, S.,"Extinction Limits of Premixed Catalyzed Flames in Stagnation Point Flows," *Combustion Science and Technology*, Vol. 48, 1986, pp. 1–30.

[3] Warnatz, J., Allendorf, M. D., Kee, R. J., and Coltrin, M. E., "A Model of Elementary Chemistry and Fluid Mechanics in the Combustion of Hydrogen on Platinum Surfaces," *Combustion and Flame*, Vol. 96, 1994, pp. 393–406.

[4] Law, C. K., Ishizuka, S., and Mizomoto, M., "Lean-Limit Extinction of Propane/Air Mixtures in the Stagnation-Point FLow," *Proceedings of the Combustion Institute*, Vol. 18, 1981, pp. 1791–1798.

[5] Ikeda, H., Sato, J., and Williams, F. A., "Surface Kinetics for Catalytic Combustion of Hydrogen-Air Mixtures on Platinum at Atmospheric Pressure in Stagnation Flows," *Surface Science*, Vol. 326, 1995, pp. 11–26.

[6] Gardner, T. J., 2001, to appear.

[7] Matkowsky, B. J., and Olagunju, D. O., "Pulsations in a Burner-Stabilized Plane Flame," *SIAM Journal on Applied Mathematics*, Vol. 40, 1981, pp. 551–662.

[8] Booty, M. R., Margolis, S. B., and Matkowsky, B. J., "Interaction of Pulsating and Spinning Waves in Nonadiabatic Flame Propagation," SIAM Journal on Applied Mathematics, Vol. 47, 1987, pp. 1241–1286.

[9] Kaper, H. G., Leaf, G. K., Margolis, S. B., and Matkowsky, B. J., "On Nonadiabatic Condensed Phase Combustion," *Combustion Science and Technology*, Vol. 53, 1987, pp. 289–314.

[10] Margolis, S. B., and Johnston, S. C., "Multiplicity and Stability of Supercritical Combustion in a Nonadiabatic Tubular Reactor," *Combustion Science and Technology*, Vol. 65, 1989, pp. 103–136.

Figure Captions

Fig. 1. Model geometry for a nonadiabatic premixed flame in stagnation-point flow. Heat loss is modelled volumetrically and is related to the surface-to-volume ratio of the combustor. Near extinction, the reaction region lies adjacent to the catalytic surface.

Fig. 2. Outer solution profiles. The curves for $\Theta^{(o)}(z;H)$ and $y^{(o)}(z;Le)$ were drawn for $H = 0.1$ and $Le = 1$, respectively.

Figs. 3a,b. Solution response in the absence of catalysis ($\alpha_2 = 0$) for reaction orders (a) $n = 1$ and (b) $n = 2$. Physical solutions (solid curve) are restricted to $-\theta_s \geq h\gamma\sqrt{\pi}/2$. A steady, planar solution does not exist for $\alpha_1 > \alpha_1^e$, where α_1^e is the extinction limit given by $\alpha_1^e = Le \cdot e^{-h\gamma\sqrt{\pi}/2}$ for $n = 1$ and $\alpha_1^e = 2Le^{3/2}e^{-h\gamma\sqrt{\pi}/2}$ for $n = 2$. The curves corresponding to $h > 0$ were drawn for $h = 2$.

Figs. 4a,b. Solution response for activation-energy ratio $\nu = 1/2$ and either (a) $2\alpha_2 Le > 1$ or (b) $2\alpha_2 Le < 1$. For $\alpha_2 > (2Le)^{-1}$, corresponding to a relatively strong surface reaction, an extension of the extinction limit to the higher value $\alpha_1^e = Le(1 + \delta + \alpha_2\delta^2 Le)\, e^{-h\gamma\sqrt{\pi}/2-\delta}$ is realized. For $\alpha_2 < (2Le)^{-1}$, corresponding to a relatively weak catalytic influence, the solution response is modified accordingly, but the extinction limit is the same as that obtained in the absence of catalysis. The curves in (a) were drawn for $\alpha_2 = 1$, while those in (b) were drawn for $\alpha_2 = 7/16$. Remaining parameter values were taken as $Le = 1$ and (for $h > 0$) $h = 2$.

Figs. 5a–e. Solution response for $\nu < 1/2$ and various values of h, Le and α_2: (a) $\nu = 0.2$, $Le = 1$ and $\alpha_2 = 0.35$; (b) $\nu = 0.15$, $Le = 1$ and $\alpha_2 = 0.35$; (c) $\nu = 0.2$, $Le = 1$ and $\alpha_2 = 0.6$; (d) $\nu = 0.2$, $Le = 0.75$ and $\alpha_2 = 0.35$; (e) $\nu = 0.2$, $Le = 1.25$ and $\alpha_2 = 0.35$. Larger values of α_2 and Le, along with smaller values of ν, have a tendency to extend the extinction limit and can thus compensate for the extinguishing effects of larger values of the heat-loss parameter h.
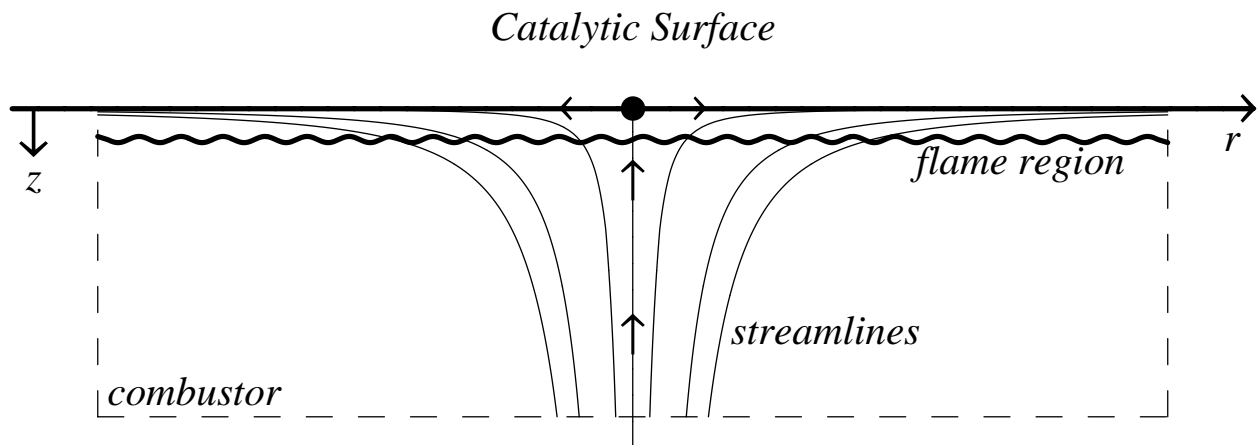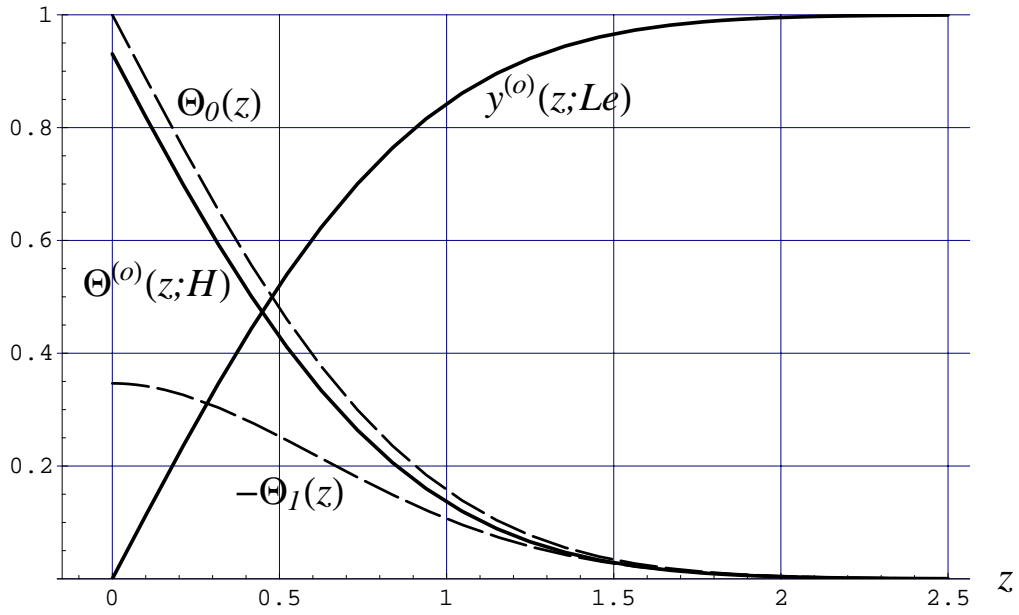
Figure 1

Model geometry for a nonadiabatic premixed flame in stagnation-point flow. Heat loss is modelled volumetrically and is related to the surface-to-volume ratio of the combustor. Near extinction, the reaction region lies adjacent to the catalytic surface.

Figure 2

Outer solution profiles. The curves for $\Theta^{(o)}(z;H)$ and $y^{(o)}(z;Le)$ were drawn for $H = 0.1$ and $Le = 1$, respectively.
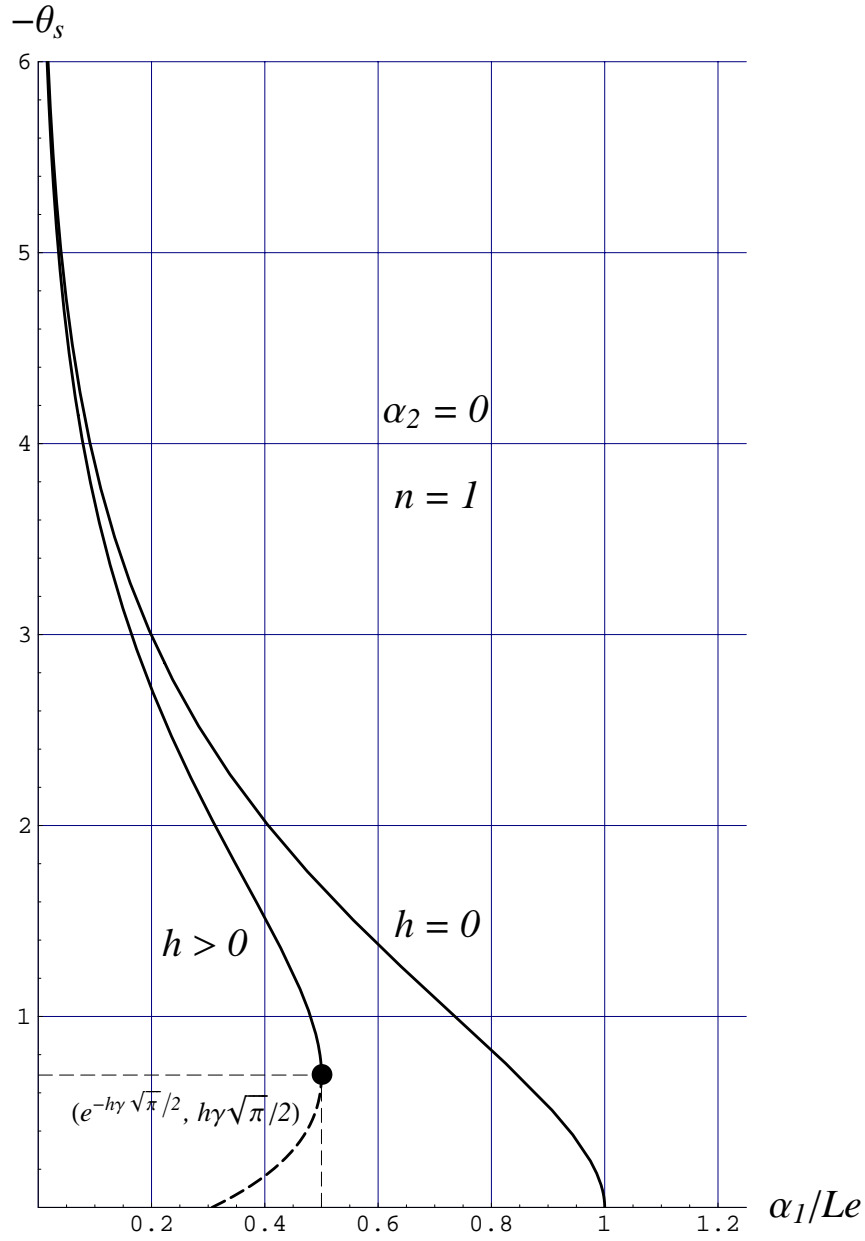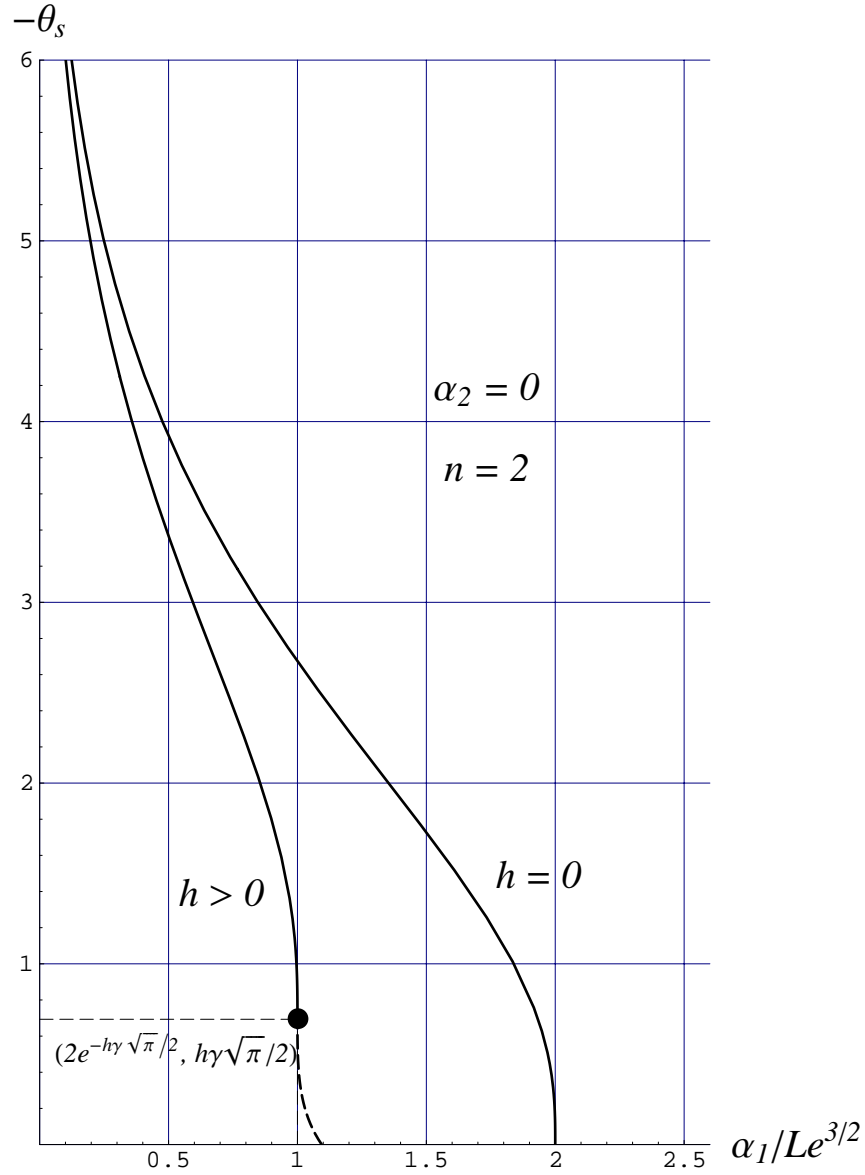
Figure 3a

Solution response in the absence of catalysis ($\alpha_2 = 0$) for reaction order $n = 1$. Physical solutions (solid curve) are restricted to $-\theta_s \geq h\gamma\sqrt{\pi}/2$. A steady, planar solution does not exist for $\alpha_1 > \alpha_1^e = Le \cdot e^{-h\gamma\sqrt{\pi}/2}$, where α_1^e is the extinction limit. The curve corresponding to $h > 0$ was drawn for $h = 2$.

Figure 3b

Solution response in the absence of catalysis ($\alpha_2 = 0$) for reaction order $n = 2$. Physical solutions (solid curve) are restricted to $-\theta_s \geq h\gamma\sqrt{\pi}/2$. A steady, planar solution does not exist for $\alpha_1 > \alpha_1^e = 2Le^{3/2}e^{-h\gamma\sqrt{\pi}/2}$, where α_1^e is the extinction limit. The curve corresponding to $h > 0$ was drawn for $h = 2$.
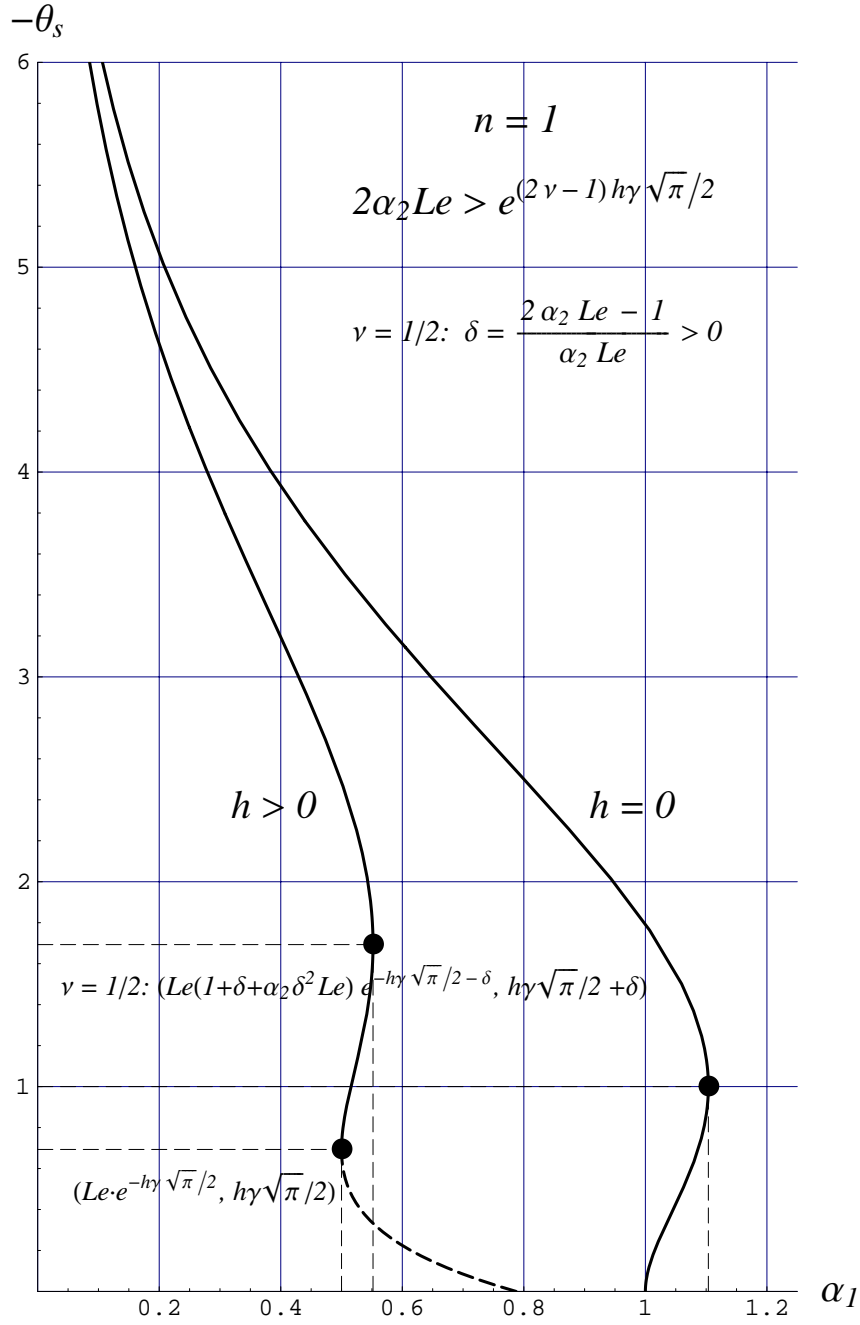
Figure 4a

Solution response for activation-energy ratio $\nu = 1/2$ and $2\alpha_2 Le > 1$. For $\alpha_2 > (2Le)^{-1}$, corresponding to a relatively strong surface reaction, an extension of the extinction limit to the higher value $\alpha_1^e = Le(1 + \delta + \alpha_2\delta^2 Le)\,e^{-h\gamma\sqrt{\pi}/2-\delta}$ is realized. The curves were drawn for $\alpha_2 = 1$, $Le = 1$ and (for $h > 0$) $h = 2$.
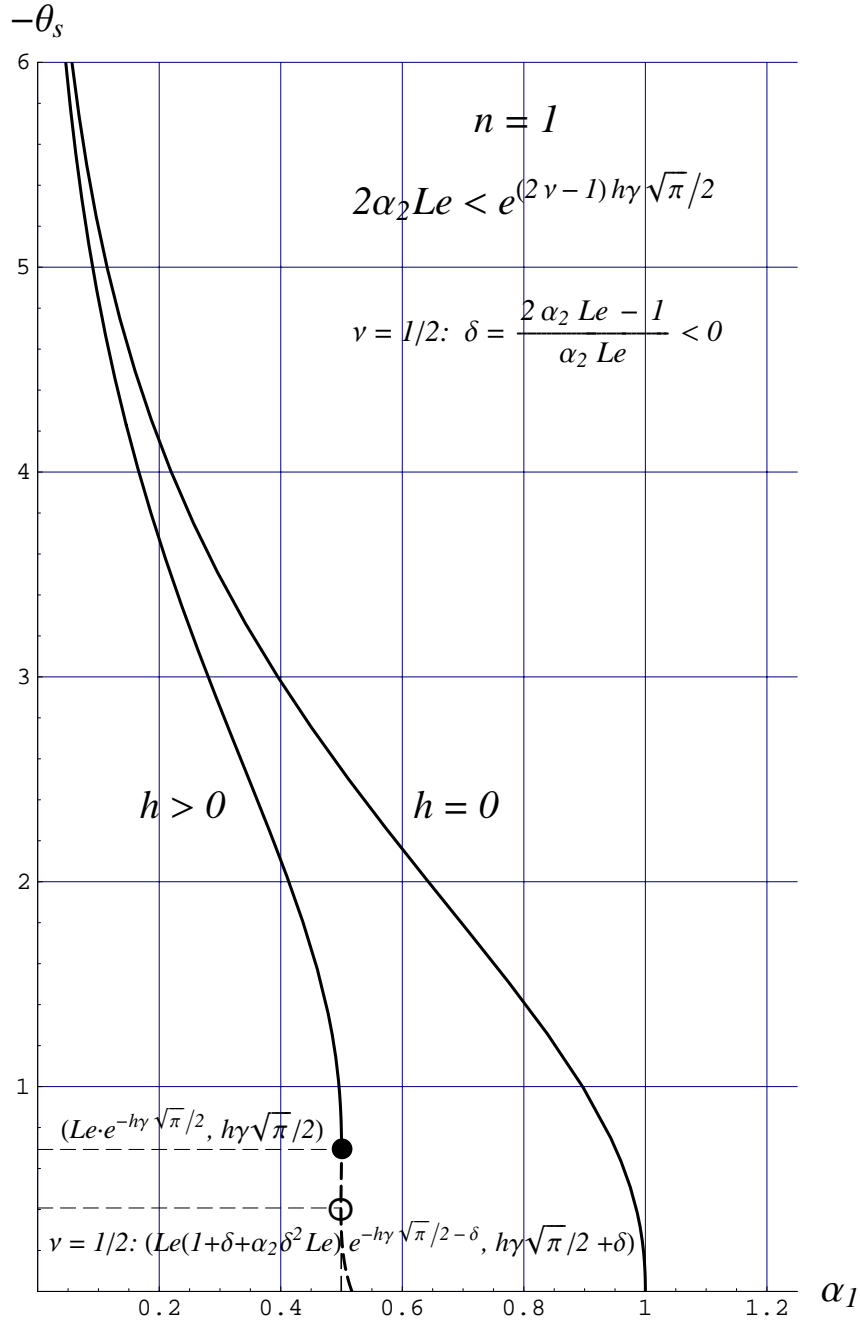
Figure 4b

Solution response for activation-energy ratio $\nu = 1/2$ and $2\alpha_2 Le < 1$. For $\alpha_2 < (2Le)^{-1}$, corresponding to a relatively weak catalytic influence, the solution response is modified accordingly, but the extinction limit is the same as that obtained in the absence of catalysis. The curves were drawn for $\alpha_2 = 7/16$, $Le = 1$ and (for $h > 0$) $h = 2$.
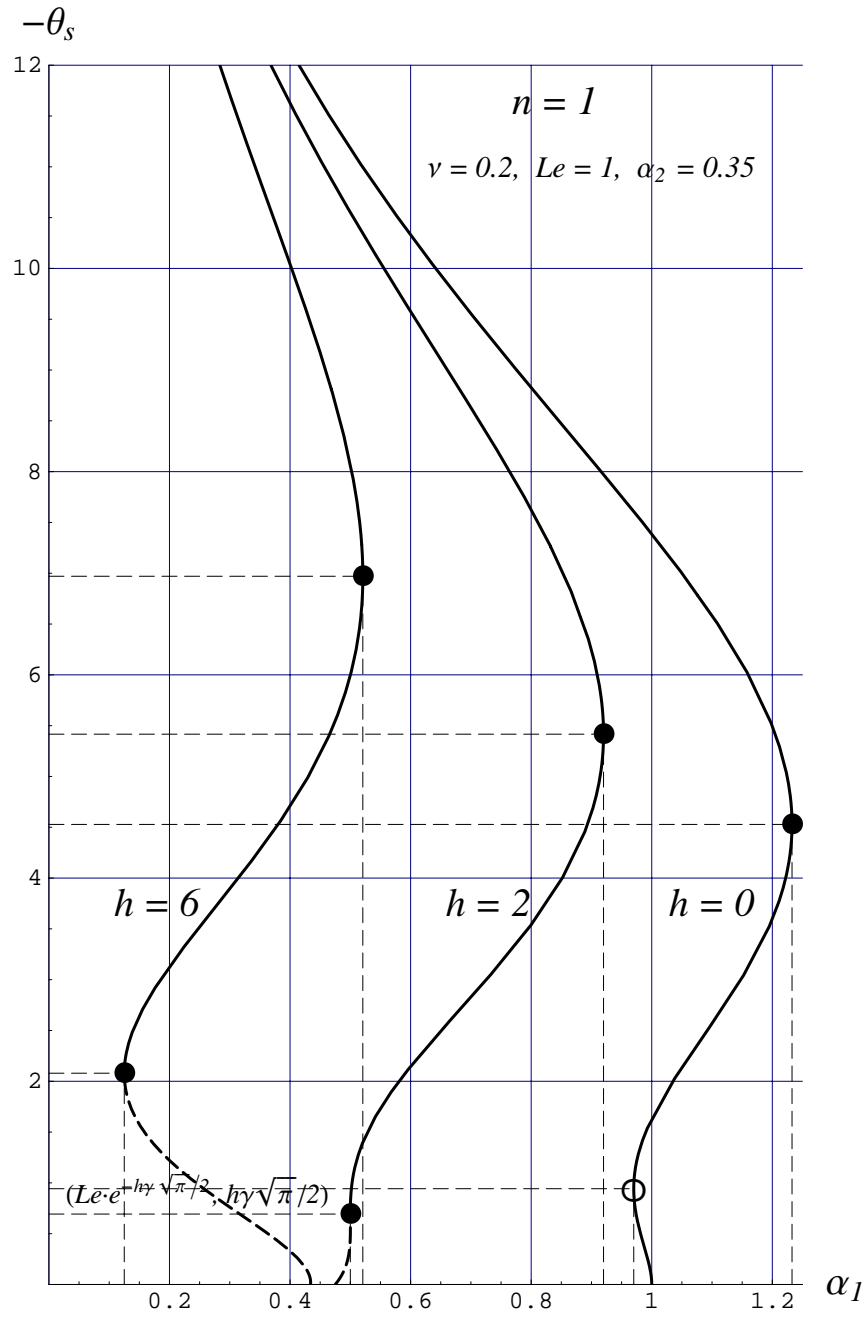
Figure 5a

Solution response for $\nu < 1/2$ and several values of h: (a) $\nu = 0.2$, $Le = 1$ and $\alpha_2 = 0.35$. Larger values of α_2 and Le, along with smaller values of ν, have a tendency to extend the extinction limit and can thus compensate for the extinguishing effects of larger heat losses.
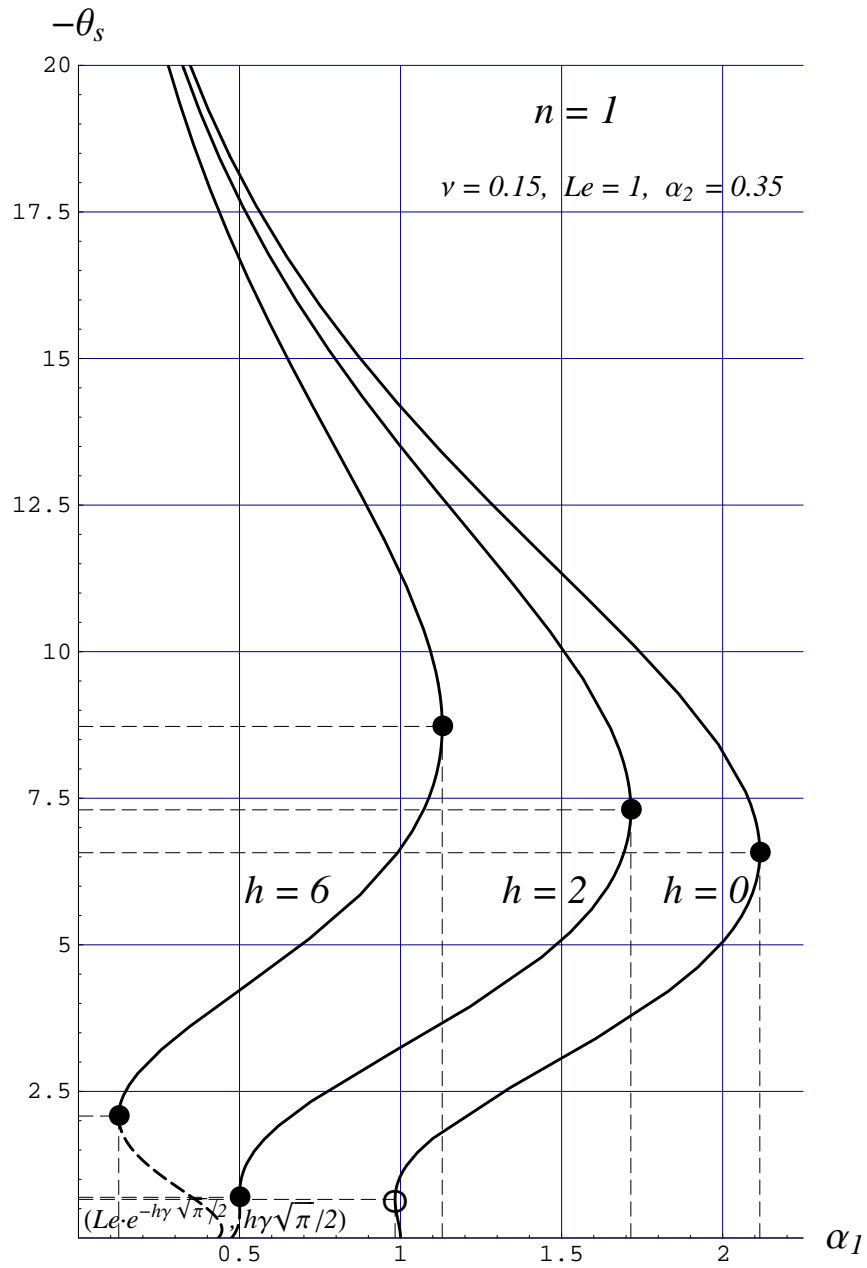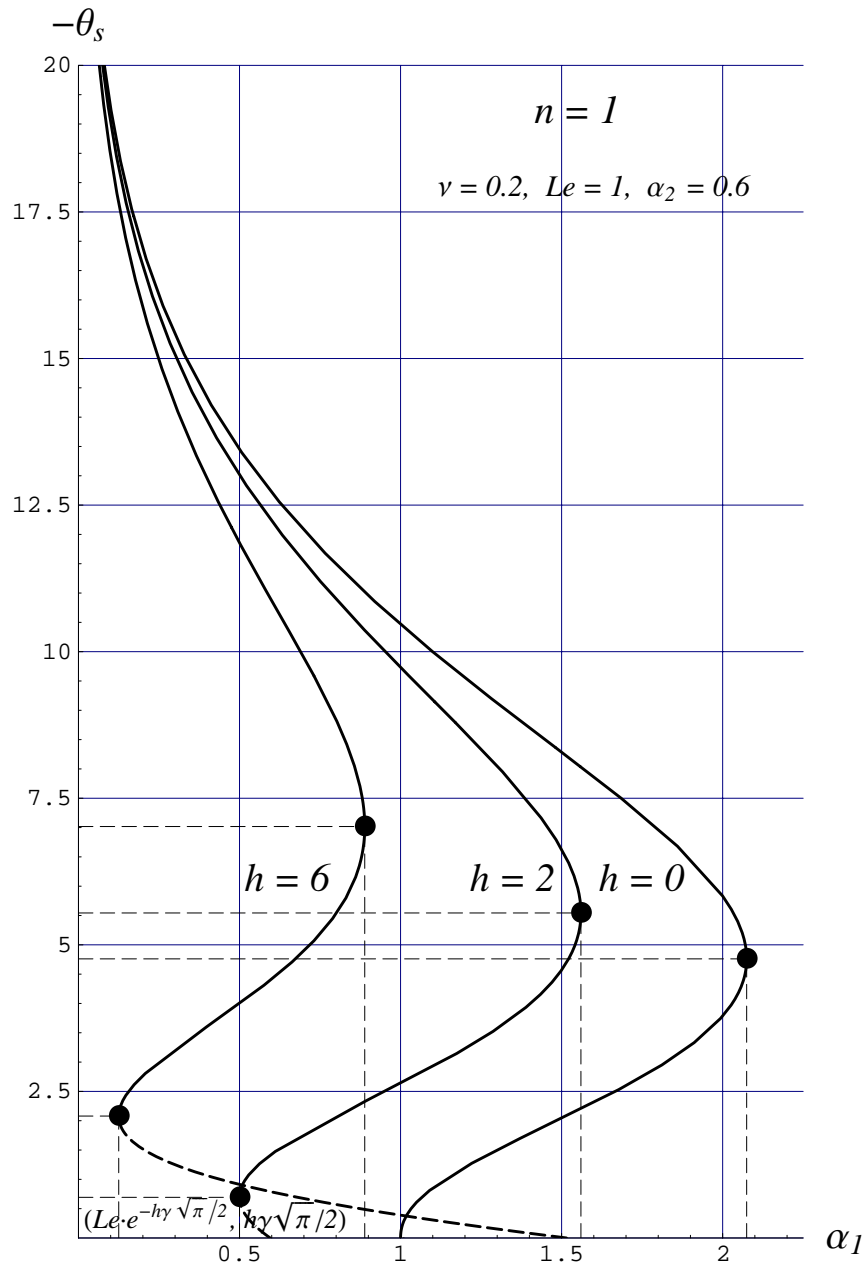
Figure 5b

Solution response for $\nu < 1/2$ and several values of h: (b) $\nu = 0.15$, $Le = 1$ and $\alpha_2 = 0.35$ Larger values of α_2 and Le, along with smaller values of ν, have a tendency to extend the extinction limit and can thus compensate for the extinguishing effects of larger heat losses.

Figure 5c

Solution response for $\nu < 1/2$ and several values of h: (c) $\nu = 0.2$, $Le = 1$ and $\alpha_2 = 0.6$. Larger values of α_2 and Le, along with smaller values of ν, have a tendency to extend the extinction limit and can thus compensate for the extinguishing effects of larger heat losses.
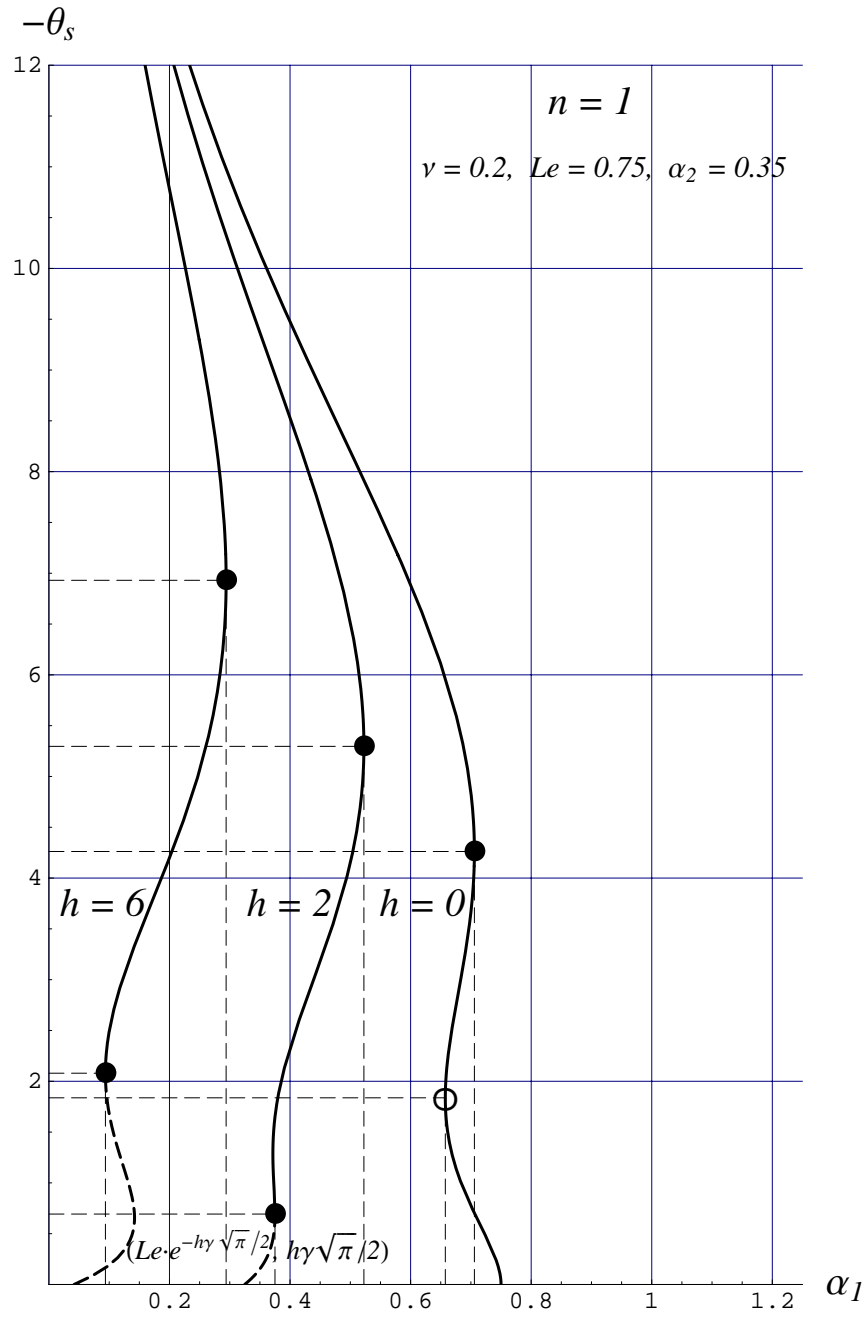
Figure 5d

Solution response for $\nu < 1/2$ and several values of h: (d) $\nu = 0.2$, $Le = 0.75$ and $\alpha_2 = 0.35$. Larger values of α_2 and Le, along with smaller values of ν, have a tendency to extend the extinction limit and can thus compensate for the extinguishing effects of larger heat losses.
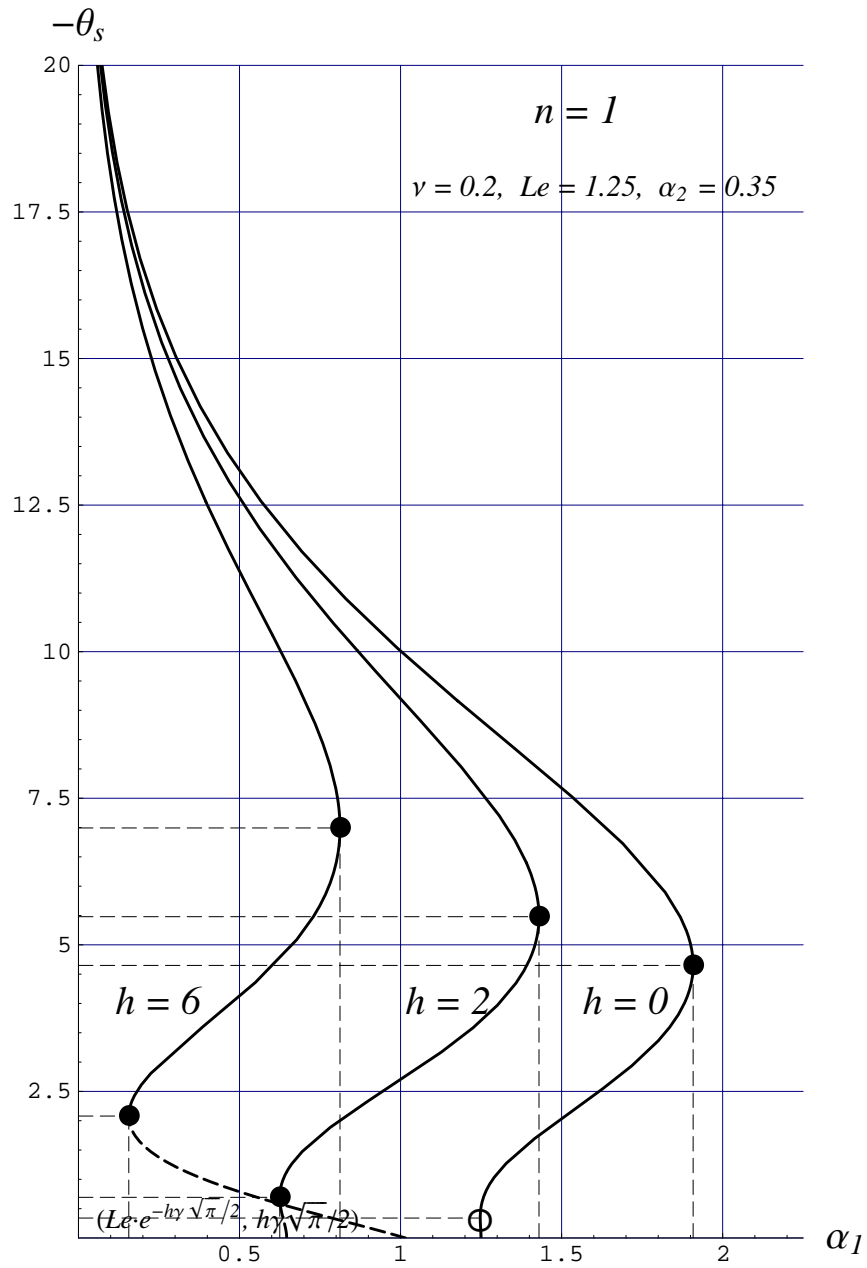
Figure 5e

Solution response for $\nu < 1/2$ and several values of h: (e) $\nu = 0.2$, $Le = 1.25$ and $\alpha_2 = 0.35$. Larger values of α_2 and Le, along with smaller values of ν, have a tendency to extend the extinction limit and can thus compensate for the extinguishing effects of larger heat losses.